Volume 11 | Number 33 | 7 September 2015 | Pages 6529–6718

Soft Matter

www.softmatter.org

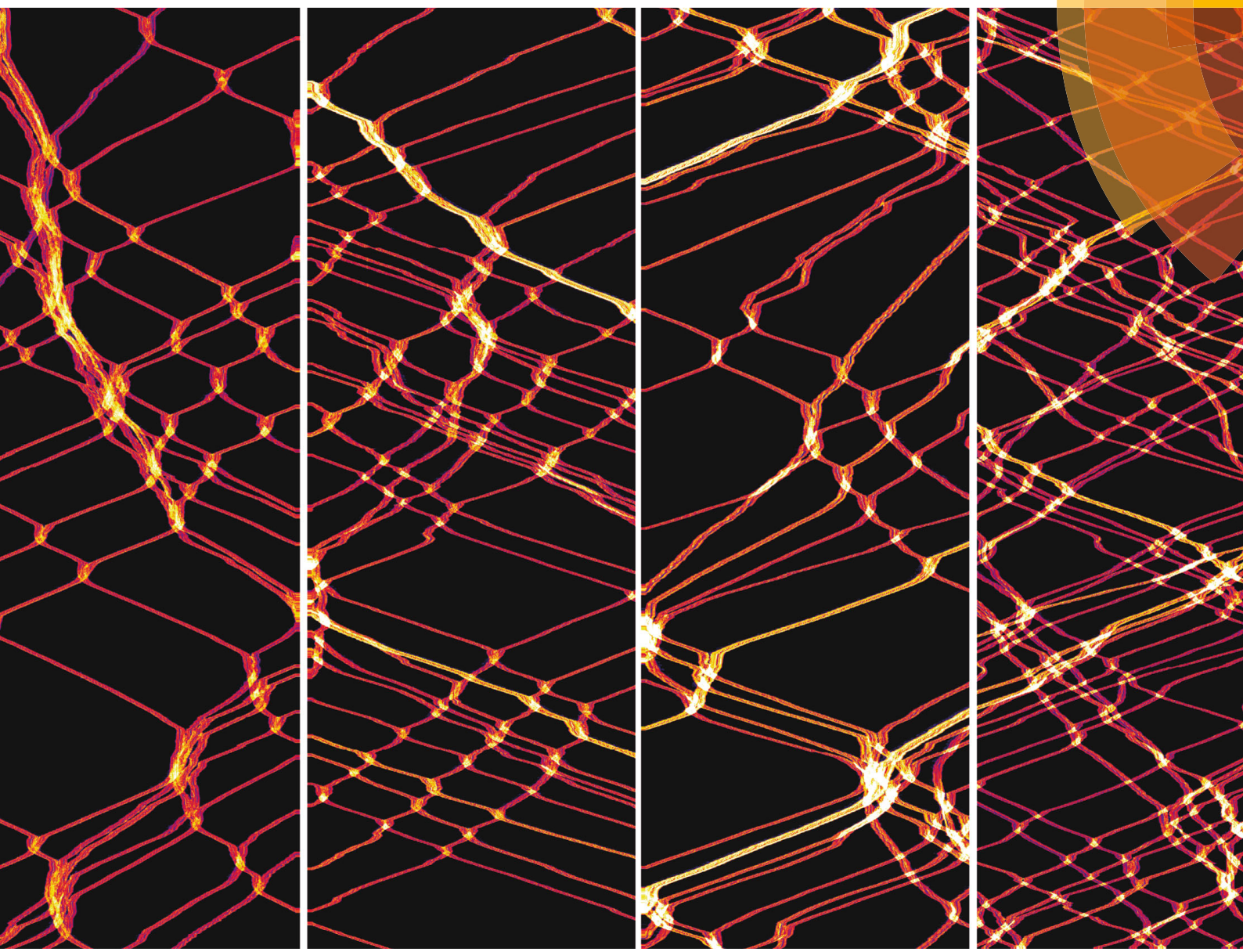

ISSN 1744-683X

ROYAL SOCIETY OF CHEMISTRY

PAPER
Nick Gravish *et al.*
Glass-like dynamics in confined and congested ant traffic

Soft Matter

PAPER

View Article Online
View Journal | View Issue

Published on 02 June 2015. Downloaded by Georgia Institute of Technology on 24/08/2015 18:36:11.

Cite this: *Soft Matter*, 2015, 11, 6552

Glass-like dynamics in confined and congested ant traffic†

Nick Gravish,*[a] Gregory Gold,[a] Andrew Zangwill,[a] Michael A. D. Goodisman[b] and Daniel I. Goldman[ab]

Received 24th March 2015,
Accepted 2nd June 2015

DOI: 10.1039/c5sm00693g

www.rsc.org/softmatter

The collective movement of animal groups often occurs in confined spaces. As animal groups are challenged to move at high density, their mobility dynamics may resemble the flow of densely packed non-living soft materials such as colloids, grains, or polymers. However, unlike inert soft-materials, self-propelled collective living systems often display social interactions whose influence on collective mobility are only now being explored. In this paper, we study the mobility of bi-directional traffic flow in a social insect (the fire ant *Solenopsis invicta*) as we vary the diameter of confining foraging tunnels. In all tunnel diameters, we observe the emergence of spatially heterogeneous regions of fast and slow traffic that are induced through two phenomena: physical obstruction, arising from the inability of individual ants to interpenetrate, and time-delay resulting from social interaction in which ants stop to briefly antennate. Density correlation functions reveal that the relaxation dynamics of high density traffic fluctuations scale linearly with fluctuation size and are sensitive to tunnel diameter. We separate the roles of physical obstruction and social interactions in traffic flow using cellular automata based simulation. Social interaction between ants is modeled as a dwell time (T_{int}) over which interacting ants remain stationary in the tunnel. Investigation over a range of densities and T_{int} reveals that the slowing dynamics of collective motion in social living systems are consistent with dynamics near a fragile glass transition in inert soft-matter systems. In particular, flow is relatively insensitive to density until a critical density is reached. As social interaction affinity is increased (increasing T_{int}) traffic dynamics change and resemble a strong glass transition. Thus, social interactions play an important role in the mobility of collective living systems at high density. Our experiments and model demonstrate that the concepts of soft-matter physics aid understanding of the mobility of collective living systems, and motivate further inquiry into the dynamics of densely confined social living systems.

1 Introduction

The natural world presents a diversity of collective biological behaviors across scales:[1] these include the transport of motor proteins,[2] the movement of cells during wound healing,[3–5] the flocking of birds,[6,7] and the migration of organisms across landscapes. In many systems, the fluid-like patterns of moving bands, swirls, and flocks of animals have motivated development of hydrodynamic and statistical mechanics descriptions for living systems.[1] These models typically incorporate close-range repulsive and long-range attractive interactions to model animal groups that are moving in unconfined open spaces.[8] For example, whirling patterns in flocking birds and fish have been explained by models of neighbor attraction based on distance or social-network.[9,10]

Collective motion of some high density living systems (cellular to human-scale collectives[11–14] and vehicular traffic[15]) can be described as supercooled fluids and/or glasses. When diverse non-living systems such as collections of grains, colloids, or molecules[16–23] are cooled or increased in density, particle mobility decreases and the relaxation timescale of the system increases.[16,24] As motion slows, heterogeneous regions of the system begin to display correlated motion (or immobility) and the system separates into dynamically mobile and immobile regions.[21,25] Eventually the size of immobile regions in the system grows and the relaxation time exceeds experimental timescales. Many previous studies have observed that traffic flows of collective systems of ants,[26] termites,[27,28] pedestrians,[29–32] and even inert granular systems[17,33] decrease in mobility as density increases. However, the underlying behavioral mechanisms which govern the traffic dynamics are largely unexplored.

[a] School of Physics, Georgia Institute of Technology, Atlanta, GA 30332, USA. E-mail: nick.gravish@gmail.com
[b] School of Biology, Georgia Institute of Technology, Atlanta, GA 30332, USA

† Electronic supplementary information (ESI) available. See DOI: 10.1039/c5sm00693g

 This journal is © The Royal Society of Chemistry 2015

Published on 02 June 2015. Downloaded by Georgia Institute of Technology on 24/08/2015 18:36:11.

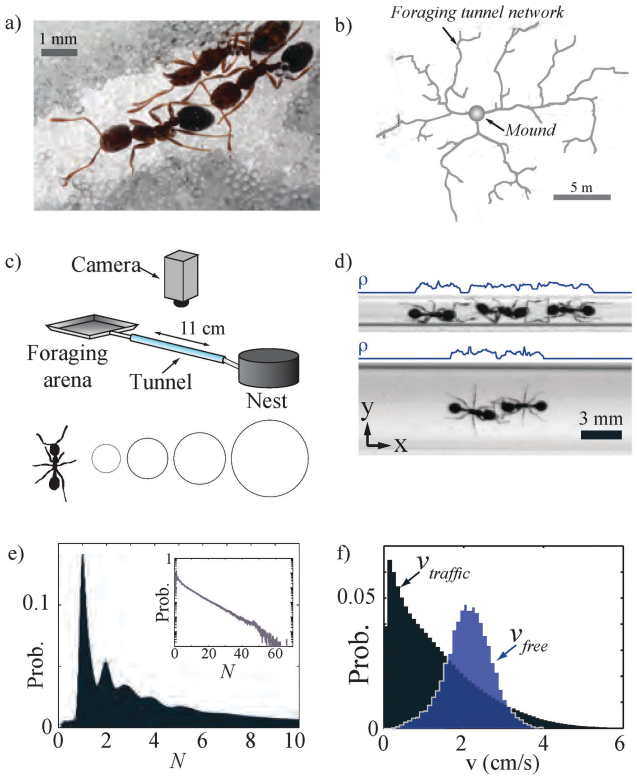

Fig. 1 (a) Fire ant workers in a tunnel. (b) Underground foraging tunnel network. Reproduced from ref. 35. (c) Schematic of experimental setup. Below, tunnel diameters and characteristic ant size. (d) Images from 2 mm (top) and 6 mm (bottom) tunnel experiments. Longitudinal tunnel density, $\rho(x,t)$ is shown above each image. (e) Probability density of number of ants in a tunnel. Inset shows same plot on a logarithmic y-scale. (f) Probability density of velocity in traffic and free flow conditions.

Confined collective movement is also common in eusocial organisms, such as ants or termites, which live in high density societies that consist of reproductive and non-reproductive colony members.[34] Eusocial insects often build complex nests composed of networks of tunnels within which they live and move (see ref. 34–36 and Fig. 1a and b). The nests ensure constant interactions which allow for transfer of information, materials (food & water), and colony members themselves (movement of brood or dead ants). Little is known, however, about how macroscopic living systems, which have complex body shapes, close-range interactions, and eusocial behavior, will respond during high density collective motion in subterranean environments.[13,15,37–39]

Ants, such as the fire ant *Solenopsis invicta*, move within the narrow crowded tunnels that comprise their nests. Moreover, fire ants build complex nests in a variety of soils[40,41] and construct underground foraging tunnels which can stretch up to 50 meters in total length (see Fig. 1b[35]). Thus the effective flow of traffic and the transport of resources over long distances (and within the more topologically complex nest) is necessary for the survival of the colony. Unlike traffic conditions confronted by surface foraging ants, such as leaf-cutter and army ants,[42–45] traffic within the nest is subject to confinement (ants cannot move off of a crowded trail). Investigation of surface-based ant traffic has revealed that ants regulate their traffic flow on narrow trails through head-on contact and pheromone based feedback mechanisms.[26,43,46,47] Thus, similar to the traffic mitigating behaviors during above ground ant foraging such as lane-formation[45] and platoons,[43,48] collective locomotion behaviors specific to subterranean traffic may also have developed to prevent jamming and clogging.

Interactions among nest-mates in eusocial societies are essential to enable information processing and resource transport. For instance, the collective foraging behaviors of seed harvester ants are determined by individuals counting the number of nest–mate interactions at the nest-entrance.[49] Additionally, the head-on encounters of leaf-cutter ants on surface foraging trails facilitate resource exchange and help to alleviate traffic jams.[26] However, it is unclear how similar behaviors and similar interactions may influence collective mobility within the dense nest environment,[34,50] and it is further unclear how soft-matter physics may inform collective animal behavior in these environments.

Inspired by these ideas, and by the seeming simplicity of the one dimensional confined traffic in linear tunnels, we use a combination of laboratory controlled studies of confined fire ant traffic and a cellular automata model to discover principles of discrete, flowing, living systems. We show that at high density collective ant flow can be described by the physics of glass-forming soft materials and that such an analogy might help provide guiding insight for the discovery of principles for active matter flow. Our cellular automata model reveals that while ants can be modeled as repulsive hard spheres, we must include ''localizing'' interactions to capture their collective behaviors.[8] These localizing interactions function similarly to attractive interactions in non-living glass-formers. Through our soft-matter motivated description of ant traffic we develop a sensitivity hypothesis to categorize the modes of clogging and means by which ant collectives may avoid it. Understanding the influence of these mechanisms on the mobility of collective animal groups has broad implications for biological group-behavior and soft-matter physics.

2 Methods

2.1 Experiment

Fire ant colonies were collected in Georgia, USA in 2011–2012. Colonies were separated from soil using the water drip method and were housed in plastic bins that contained an enclosed nest area made from petri dishes and an open foraging arena. We provided insects to the colonies as food and water *ad libitum*. We monitored unperturbed traffic between a laboratory nest and an open foraging arena (Fig. 2a and Videos 1 and 2, ESI†). The foraging arena consisted of a 27 cm × 17 cm plastic bin with Fluon coated walls in which we placed a constant supply of water and food. A lamp placed above the arena illuminated and heated the foraging zone. A plastic tube connected the foraging arena to a glass tunnel oriented horizontally with varied diameter (D = 2, 3, 4, 6 mm) and length, L, of 11 cm (Fig. 1c). The glass

Published on 02 June 2015. Downloaded by Georgia Institute of Technology on 24/08/2015 18:36:11.

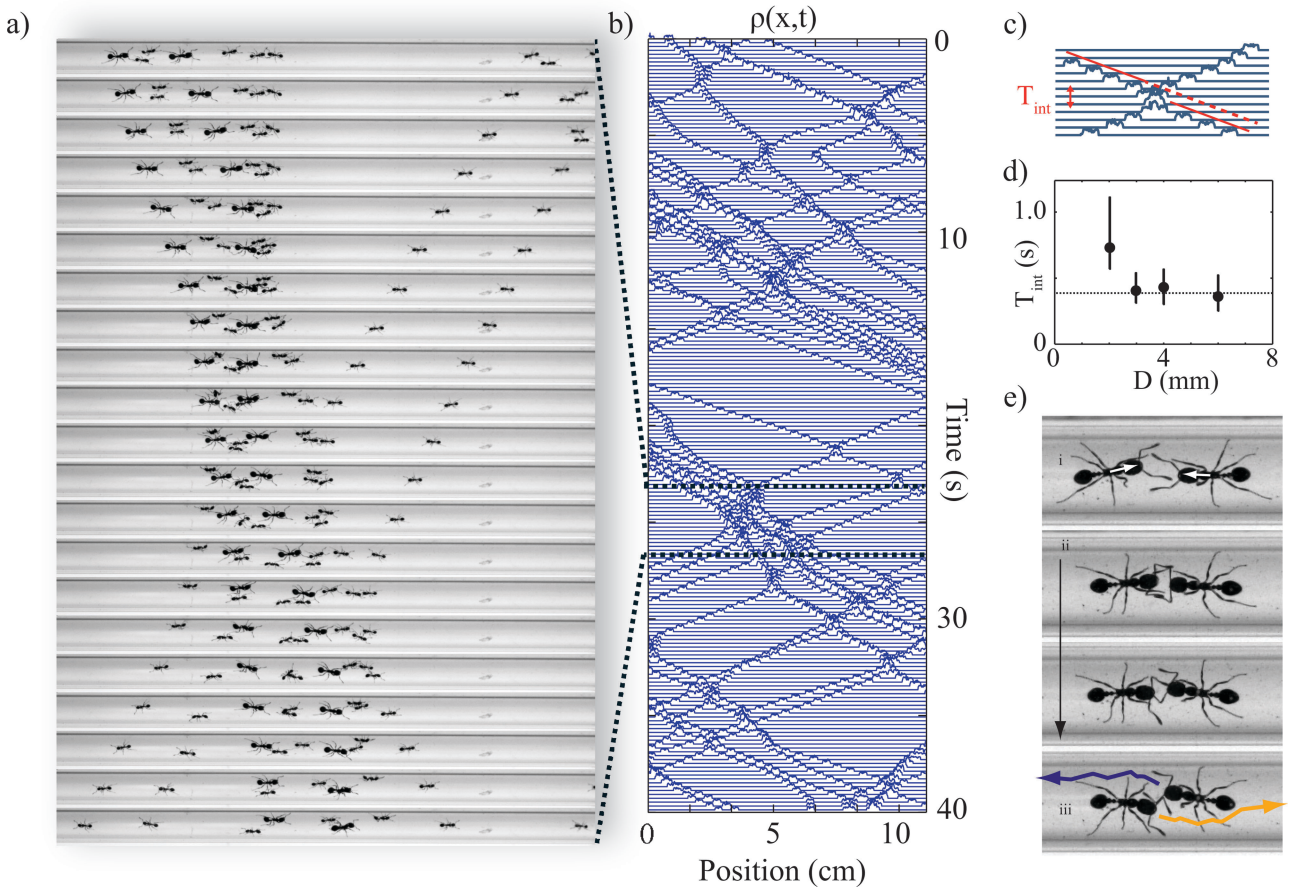

Fig. 2 Space-time diagram of ant–traffic and ant–ant interactions. (a) Image sequence of ants moving bi-directionally in a 6 mm tunnel. Images are separated by 0.18 s and tunnel length is 10 cm. (b) Spatio-temporal evolution of the one-dimensional tunnel density, $\rho(x,t)$. Curves are offset vertically in time downwards. (c) Spatio-temporal evolution of tunnel density during an interaction between two ants. Red line highlights the trajectory before and after interaction, and dashed line shows the trajectory if no interaction had occurred. (d) Characteristic interaction times in four different tunnel diameters. Dashed line is T_{int} = 0.45 ± 0.26 s. (e) Ant–ant interaction in a 4 mm tunnel showing antennation. Time between frames is 0.25 s.

tunnel was connected to an enclosed plastic nest which was painted black and contained a moist plaster-of-paris floor.

Five separate groups of 500–2000 worker fire ants of body length 3.5 ± 0.5 mm were removed from their host colony and placed in the foraging arena. We excluded queens, males, and brood from the group. The five worker groups were drawn from three colonies and each group was monitored in independent experiments over the course of three months. Within several hours of relocation to the foraging arena, the workers migrated to the nest and maintained a continuous flow of bi-directional traffic from the nest to the foraging arena and back. We monitored the foraging traffic of worker groups for 24–72 hours within each of the four tunnel sizes. The order of tunnel presentation to the worker group was randomized across different group trials.

We recorded video sequences of traffic; recordings were 40 seconds in duration at a rate of 100 Hz, and resolution of 100 × 1328 pixels (120 pixels was equal to 1 cm). After the collection of each video we performed post-processing in Matlab which consisted of dividing each video frame by a stationary background image and thresholding the resultant image to generate a binary image time-series, where $I_t(x,y)$ is the experimental image at time t. Following image processing a new video was captured. The time interval between successive videos was ≈2 minutes. In summary, our experiment consisted of over 10 000 videos each with 4000 images of trafficking ants.

We analyzed spatio-temporal traffic dynamics as a one-dimensional flow of longitudinal density, $\rho(x,t)$ along the length of the tunnel, x (Fig. 1d). $\rho(x,t)$ is defined as $\rho(x,t) = \sum_y I_t(x,y)$. We define the number of ants within a tunnel as $N(t) = C\sum_x \rho(x,t)$ where $\sum_x$ is the sum over the entire length of the tunnel, and C is a normalization constant chosen such that $N(t) = 1$ when one ant is in the tunnel (see histogram in Fig. 1e). The longitudinal average global tunnel density is defined as $\rho_G = N/L$. Often, when two or more ants approached each other, they stopped and briefly interacted through antennation before moving along their respective paths. To quantify this interaction behavior, we hand-tracked ants during bouts of antennae contact and measured the duration of these interactions (see Fig. 2c–e). We define the interaction time, T_{int}, as the time from first antennae contact between two ants to the time when they have passed and their petioles are aligned.

 This journal is © The Royal Society of Chemistry 2015

Published on 02 June 2015. Downloaded by Georgia Institute of Technology on 24/08/2015 18:36:11.

2.2 Simulation

To gain insight into the behavioral and physical contributions to the observed traffic flow, we implemented a 2D cellular automata model in which we input interaction rules inspired by experimental observation, and studied the resultant ant traffic (Fig. 3). In our model, ants occupied lattice sites on a square-lattice grid and moved bi-directionally along the tunnel length with either straight or diagonal steps along the direction of travel. We considered ant–ant interactions as causing a short time-delay to the participating individuals motions. This mode of interaction is different from previous modeling approaches of collective motion, such as those of bird flocks or fish schools, in which interactions are modeled as some combination of attractive and repulsive potentials.[1] Ants entered the tunnel from the left or right at random and advanced along a direction of motion towards the opposite tunnel end. Ants advanced forward by one lattice site during each iteration; however only a single ant occupied a lattice site at one time. Two ants adjacent to each other in the head-on direction were permitted to move only by jumping diagonally to an open lattice site with probability p.

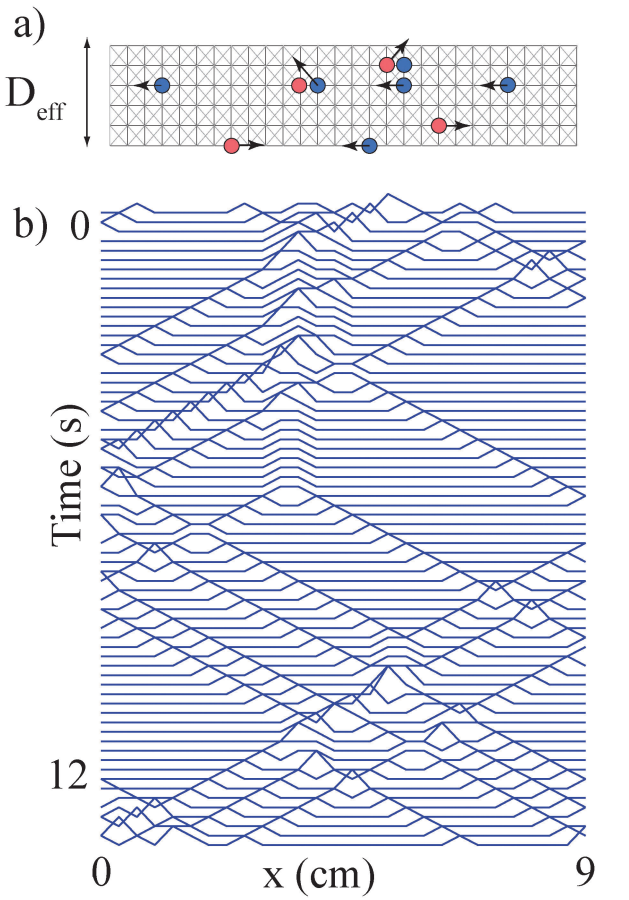

Fig. 3 Schematic of simulation geometry and space-time results. (a) Simulated ants move left or right along square lattice with diagonal connectivity and move around each other through diagonal steps. (b) Space-time plot of simulated trajectories where height at each row indicates longitudinal density.

By varying p we could vary the interaction time, T_{int}, in the simulation to explore how head-on encounters influenced traffic. The probability for a head-on encounter to terminate is given by the combined probability of either ant jumping past each other, $2p - p^2$. The statistics of head-on encounters in experiment follow a Poisson process and thus the interaction time between two ants in the simulation was determined from the median value of the exponential distribution function. The median interaction time of ants in the simulation with time-step $dt = 0.175$ s is $[\ln(2)/(2p - p^2)]dt$. We fixed the length of the simulated tunnel to match that of the experiment with tunnel length $l = 31$ L and grid-length of one bodylength. The time step of the simulation ($dt = 0.175$ s) was chosen such that the free-speed was 2 cm s^{-1}, matching experiment. We varied the width of the tunnel from D_{eff} = 3–100 lattice spaces. In simulations studying the fragile-strong glass formation we performed simulations in D_{eff} = 10 tunnels with periodic entrance and exit boundary conditions to fix average density.

3 Results & discussion

3.1 Traffic and interactions

We observed fire ant foraging traffic within tunnels of diameter ranging from 2–6 mm over periods of days for each tunnel diameter. Ants maintained bi-directional traffic in all tunnel diameters. From automated tracking of the velocity of ant aggregations within the tunnel we computed speed distributions for scenarios in which ants moved in traffic, and in which they moved freely through the tunnel. We observed that the free speed distribution (when only a single ant was present in the tunnel) was roughly Gaussian distributed with $\langle v_{free} \rangle = 1.93 \pm 0.63$ cm s^{-1}. The speed distribution when more than one ant was in the tunnel was skewed to the right with the majority of speeds near zero (Fig. 1f).

The motion of an individual ant was interspersed with bouts of free running and stationary interactions with other ants (Fig. 2a and b) as they moved to or from the nest site. U-turns were infrequent (approximately less than 10% of trajectories) and were not considered in our analysis. Stationary aggregations of ants often nucleated and persisted within the tunnels as shown in the space-time image of Fig. 2b. A fundamental observation of ant traffic is that independent of the available space to maneuver, ants routinely stopped to interact with each other (Fig. 2c–e). Ants antennated during head-on encounters which is a primary mechanism of tactile information acquisition.[34] We measured the interaction time between ants (T_{int}) and observed that in tunnel diameters larger than 2 mm $T_{int} = 0.45 \pm 0.26$ s (Fig. 2d). In contrast, the 2 mm tunnel interaction times were skewed to longer durations, with a mean value of $T_{int} = 1.13 \pm 1.30$ s. This difference is likely due to the reduced lateral space which altered the duration over which ants crossed paths.

From a behavioral perspective, halting to interact with other ants in the tunnel serves an important biological function that enables eusocial insects to acquire information about foraging

Published on 02 June 2015. Downloaded by Georgia Institute of Technology on 24/08/2015 18:36:11.

resources,[51] colony state,[28] and intruders. However, these stationary interactions within the tunnel have the potential to cause large-scale aggregations and traffic jams, which can be detrimental to resource flow. To address the decrease in mobility associated with local density fluctuations we next measured the mobility of individuals within the tunnel.

3.2 Traffic statistics

We characterized the mobility statistics in experiment and simulation through measurement of the occupancy and vacancy time of sites within the tunnel (Fig. 4a). The vacancy time is the time interval that a site along the tunnel length, x, is unoccupied (*i.e.* $\rho(x,t) = 0$). The occupancy time is the duration that the site is occupied by an ant (*i.e.* $\rho(x,t) \neq 0$). Vacancy and occupancy time distributions for the four tunnels were insensitive to tunnel diameter (Fig. 4b and c). Vacancy distributions were broadly distributed with an exponential tail (Fig. 4b) indicative of a Poisson waiting process for site occupations. However, the occupancy time distributions did not display an exponential decay and instead were better described with a power law tail (Fig. 4c) with a roughly -3 scaling exponent. The distribution of occupancy time among all tunnels had similar peak locations at a time of $\frac{\text{bodylength}}{v_{\text{free}}} \approx \frac{0.35\ \text{cm}}{1.9\ \text{cm s}^{-1}} \approx 0.18$ s – the occupation time of freely moving ants.

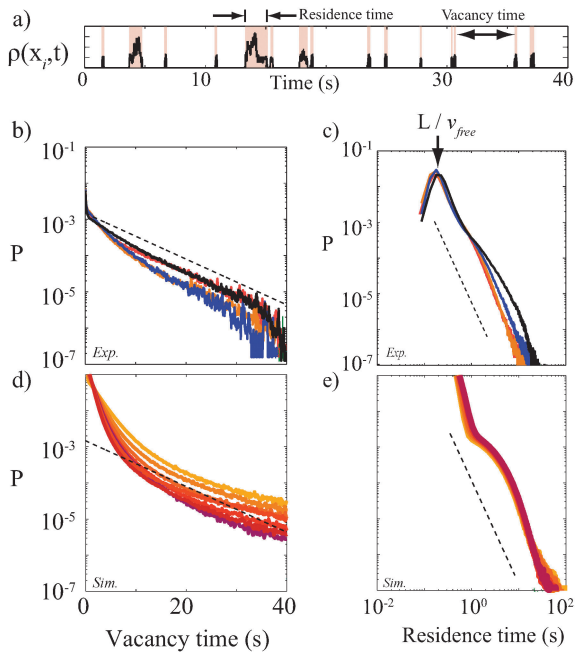

Fig. 4 Probability distribution of the site vacancy times in experiment and simulation. (a) Example of $\rho(x,t)$ at fixed location in space (x_i) over time. Annotations highlight vacancy and residency times. (b) Vacancy time distribution in experiment. Colors correspond to varied tunnel diameter, D, with 2 mm black, 3 mm blue, 4 mm red, 6 mm orange. Dashed line shows exponential decay with time constant of 8 s. (c) Probability distribution of the site occupancy time in experiment. Colors same as in (b). Dashed line is a power-law with exponent of -3. (d) Vacancy time distribution in simulation. Diameter increasing from D = 3–10 from light to dark. (e) Residence time in simulation. Dashed line is same as in (c).

We did not observe differences in occupancy and vacancy time distributions in tunnels of different diameters despite differences in ant–ant interaction times; this was likely due to variation in traffic density as a function of tunnel diameter. Local density alters traffic flow speeds differently in different tunnel diameters. We measured the relationship between individual speed and local density (Fig. S1 and S2, ESI†) which is typically used to characterize vehicular and pedestrian traffic.[13] We found that, in all cases, speed monotonically decreased with increasing density, and that the traffic flux (product of speed and density) displayed a maximum at intermediate density called the carrying capacity density. The upper limit of traffic flow curves differed as a function of diameter with the 2 mm diameter flow-speed curves decreasing most rapidly with increasing density. The carrying capacity increased approximately linearly with tunnel diameter (Fig. S2, ESI†) similar to results from pedestrian traffic flow.[52]

The experimental results were well captured by the cellular automata simulation in both the density-speed relationship (Fig. S1 and 2, ESI†) and vacancy and occupancy time distributions (Fig. 4d and e). Similarity between simulation and experiment suggest that this simple kinetically constrained model consisting of excluded volume and finite time-delay interactions is sufficient to understand the basic statistics of motion within the tunnel.

3.3 Spatio-temporal dynamics of aggregations

To quantify the spatial and temporal structure of ant traffic we located all connected non-empty regions in the space-time density which we define as "aggregations". Spatially connected regions of $\rho(x,t)$ correspond to aggregation sizes of $n = \int_{x_0}^{x_f} \rho(x,t)$ where x_0, x_f are the initial and final positions of the connected aggregation respectively. The number of ants in an aggregation divided by the longitudinal-length of the aggregation represents the local density of that aggregation, $\rho_L = n/L$.

The distribution of ρ_L across all aggregations was similar between the four tunnel diameters in experiment (Fig. 5). The shape of $P(\rho_L)$ was Gaussian at small ρ_L with an exponential tail for all four tunnel diameters. The peaks at $\rho_L \approx 1.75$ ants per bodylength are likely instances of single ants or tandem aggregations. The exponential tail in $P(\rho_L)$ represents the presence of large contiguous aggregations in the traffic flow. The distribution tails suggest that at smaller tunnel diameter there is a smaller probability to observe high-density aggregations. Similar phenomena have been observed in the length distribution hard spheres (or rods) moving collectively in long strings upon transition to the glass transition.[53,54]

To gain insight into the temporal fluctuations of the tunnel density, we used a measure of mobility typically applied to non-biological dense soft-matter systems.[55–57] For each aggregation of size n (binned in increments of 0.5) we computed the density overlap correlation function.

$$Q_n(\tau) = \frac{\langle \rho(x,t_0)\rho(x,t_0+\tau)\rangle - \langle \rho(x,t_0)\rangle^2}{\langle \rho(x,t_0)^2\rangle - \langle \rho(x,t_0)\rangle^2} \quad (1)$$

which has previously been used to study dynamical heterogeneities in colloids[55] and granular materials.[57] $Q_n(\tau)$ is a

 This journal is © The Royal Society of Chemistry 2015

Published on 02 June 2015. Downloaded by Georgia Institute of Technology on 24/08/2015 18:36:11.

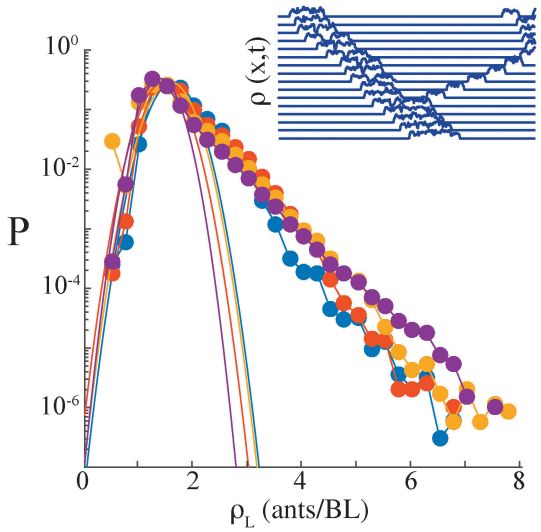

Fig. 5 Probability distribution of aggregation density in experiment. Colors are tunnel diameters, D = 6 mm purple, 4 mm yellow, 3 mm red, 2 mm blue. Solid lines are gaussian fits to the low density regime highlighting the exponential tails in aggregation. Inset shows the onset of an aggregation as three ants approach the central region of the tunnel from left and right, with time increasing down the figure.

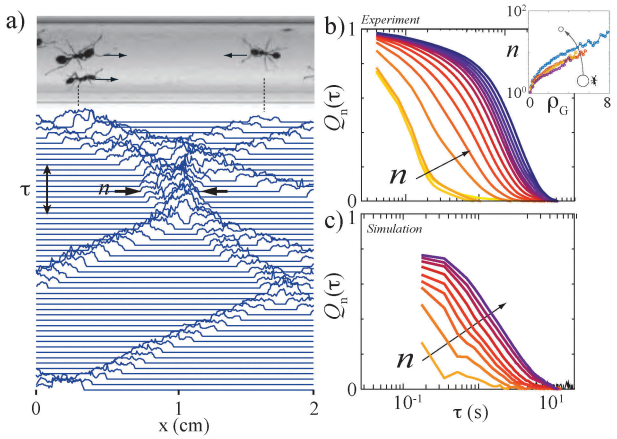

Fig. 6 Ant traffic jam dynamics investigated with the density correlation function. (a) Image of four ants approaching each other in a 6 mm tunnel. Below is shown the spatiotemporal evolution of $\rho(x,t)$ with a jam duration shown by the vertical black line. (b) Correlation function of traffic jam duration *versus* time for the 2 mm tunnel in experiment. (c) Correlation function for simulation. Curves of different color correspond to different size traffic jams with increasing n from 2–15 shown by the arrow from left to right for both (b) and (c). Inset in (b) experiment shows scaling of n *versus* the global tunnel density (in units of ants per bodylength).

function which varies from 0 to 1 measures the spatial overlap of an ant's position as a function of time lag. If ant aggregations decay slowly, the spatial overlap is high and thus $Q_n(\tau)$ remains large for longer time durations than when compared to free-flow. The brackets $\langle\cdots\rangle$ are the spatio-temporal mean of the function over the aggregation size and time interval $\tau \in [0, 13\ \mathrm{s}]$. For the calculation of $Q_n(\tau)$ we evaluated every fourth video frame to speed up computation. The correlation function interval was chosen to be long enough such that $Q(\tau) = 0$ for long time intervals.

The correlation function $Q_n(\tau)$ associated with traffic aggregations of size n thus measures how quickly high density traffic-fluctuations returned to steady flow. The $Q_n(\tau)$ curves decreased from 1 to 0 over time scale τ^* which varied with tunnel diameter and jam size (Fig. 6). We measured τ^* by fitting a stretched exponential function, $Q_n(\tau) = \mathrm{e}^{\left[-\left(\frac{\tau}{\tau^*}\right)^{\beta}\right]}$ where β is a fit parameter of order unity. For fixed tunnel diameter (D), curves of larger n were shifted to the right indicating that τ^* increased with aggregation size. Comparing $Q_n(\tau)$ curves of similar n across D indicates that τ^* increased with decreasing D.

The size of ant aggregations, n, grew approximately exponentially with increasing global density, ρ_G, within all tunnels (inset Fig. 6b). The rate of increase in ant aggregations was similar across all tunnels as a function of ρ_G.

3.4 Effects of tunnel diameter

The correlation curves in Fig. 6 are similar to many other observations of slowing relaxation in soft-matter glassy systems[25,56,58] where heterogeneous mobile and immobile regions form. The relaxation time of ant aggregations in experiment (as measured by τ^*) increased approximately linearly with increasing n for all tunnel sizes (Fig. 7). We contrast these results to those of dry granular materials[57] and colloids[55] in which τ^* is more sensitive to heterogeneity size, scaling approximately as $\tau^* \propto n^3$. That is, aggregations of ants relax more quickly than would be expected of inert soft-matter. The linear dependence of τ^* on heterogeneity size suggests that different relaxation processes that may occur in *active* systems such as the one studied here.

The slope of τ^* as a function of n can be also interpreted as a measure of how sensitive traffic flow is to the formation of jams from intermittent density fluctuations. We fit lines to τ^* *vs.* n and observed that the normalized slope of $\Delta\tau^*(n)$ (normalized such that $\lim_{D\to\infty} \Delta\tau^* = 1$‡) increased with decreasing tunnel diameter (Fig. 8a). We define $\Delta\tau^*$ as the aggregation time susceptibility. We fit $\Delta\tau^*$ *vs.* n with a function of the form $\frac{A}{(D - D_C)^{\gamma}} + 1$ (which was also chosen to describe simulation results). Aggregation time susceptibility diverged at a tunnel diameter of 1.47 ± 0.2 mm in experiment, which is approximately two-times the 0.8 mm mean head width of a fire-ant worker (Fig. 8a). The analysis of aggregation time susceptibility thus predicts that bi-directional traffic-flow is not possible in the limit that two ants cannot pass each other in a tunnel, a result that is surely to be the case in natural tunnels.

The divergence of $\Delta\tau^*$ indicates that as tunnel diameter decreases traffic flow becomes increasingly sensitive to tunnel density. The system behavior at large and small D is consistent with predictions for dense and dilute cases: in the small D (dense) regime interactions are enforced among all ants because

‡ Under our space-time representation of traffic, the width of an aggregation of n ants scales linearly with n, independent of interactions and thus we normalize the slope, $\Delta\tau^*$, to 1 to remove this effect.

Published on 02 June 2015. Downloaded by Georgia Institute of Technology on 24/08/2015 18:36:11.

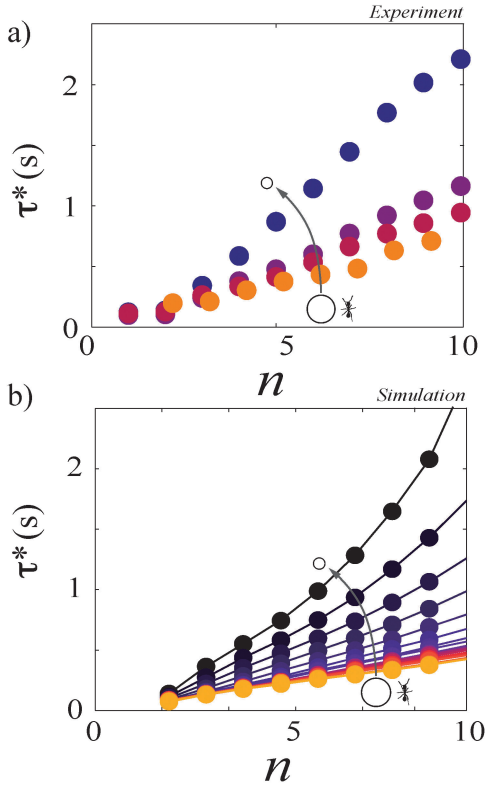

Fig. 7 Traffic jam correlation time as a function of n for increasing tunnel diameter (arrow) in experiment (a) and simulation (b). Colors correspond to tunnel diameter increasing from large to small as shown by arrow.

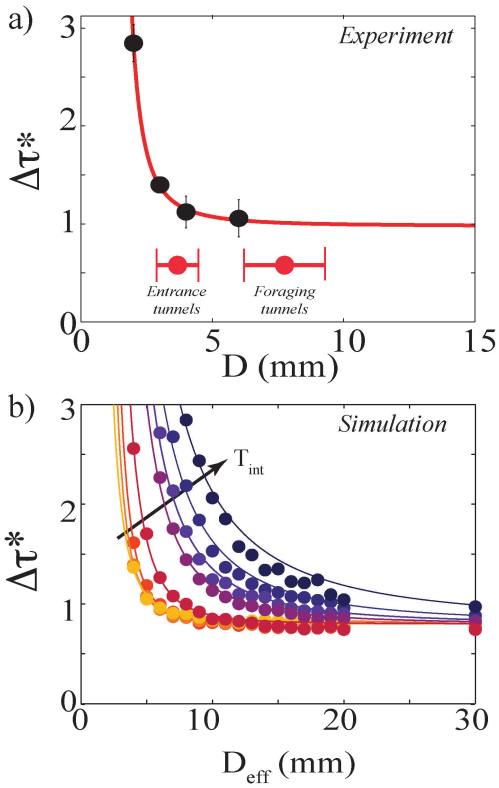

Fig. 8 Sensitivity of the slope of τ^* *versus* n (Fig. 7) as a function of tunnel diameter. (a) Results from experiment. Red curve is fit function $\frac{A}{(D-D_c)^{\gamma}}+1$ described in text. Red points with bars show diameter of foraging and entrance tunnels (Foraging tunnels from ref. 59, entrance tunnels in lab from ref. 60 and field from ref. 35). (b) Results in simulation. Different points and curves correspond to simulations with different interaction times. Arrow indicates increasing T_{int}.

of spatial limitations and thus additional workers necessarily decrease mobility, in the large D (dilute) regime the addition of workers does not significantly affect relaxation time. In the intermediate regime we see that the effect of social-interaction influences the relaxation dynamics of worker aggregations and that this process is sensitive to tunnel diameter. In simulation we are able to explore the effect of ant–ant interaction behavior on the divergence of traffic susceptibility (Fig. 8b). We find that increasing T_{int} in simulation results in a more gradual increase of $\Delta\tau^*$ *versus* D_{eff}. Thus, these results suggest that tunnel diameter in combination with innate behaviors (individual mobility and interaction times) affect the spatio-temporal traffic dynamics.

We can address the question of whether fire ant traffic is susceptible to traffic jams in natural nests by examining the $\Delta\tau^*$ curve in relation to the size of tunnels in natural nests (Fig. 8a). From measurements of the cross-sectional area of fire ant foraging tunnels,[59] we estimate the effective diameter of horizontal foraging tunnels in nature to be, $D = 7.8 \pm 1.9$ mm (tunnels are elliptical in cross-section with eccentricity of 2, see ref. 35). Vertical nest entrance tunnels in natural nests were reported in the range of 3–4 mm in diameter and a laboratory X-ray study found that vertical tunnels were $D = 3.7 \pm 0.8$.[60] Aggregation time susceptibility, $\Delta\tau^*$, is a diverging function with decreasing diameter and predicts that bi-directional traffic should be impossible in tunnels smaller than $D_c = 1.47$ mm. This minimum tunnel diameter is consistent with a previous study of climbing in tunnels in which velocity dropped to zero near this tunnel size.[60] However, over the range of natural tunnel diameters $\Delta\tau^*$ is relatively flat (Fig. 8a). Thus fire ants build tunnels that allow for effective movement and flow under normal conditions.

Our observations of traffic regulation differ from those of above ground foraging traffic in the ant *Leptogenys processionalis* in which the absence of a "jammed-phase" has been observed.[43] In previous studies the lack of observable traffic jams has been attributed to interaction behaviors like lane-formation and platoon formation.[26,45] Thus we have found that, in addition to behavioral adaptations which some ant species posses to mitigate traffic jams along trails (see ref. 48 for review), environmental modification may also enable smooth traffic flow. A similar result was observed in the construction of termite tunnels, whose width increased linearly with the number of termite workers queued up at the digging site.[28] Further experiments are needed to determine the relationship between tunnel morphology and local traffic-flow conditions.

3.5 Sociality leads to strong glass formers

We now cast our results in the framework of glass-transition physics[24] to discuss how traffic fluctuations and jams are analogous to the slowing and arrest of fragile glassy systems.

 This journal is © The Royal Society of Chemistry 2015

Published on 02 June 2015. Downloaded by Georgia Institute of Technology on 24/08/2015 18:36:11.

The language and concepts of glass-transition physics provides a convenient framework to explore collective behaviors of complex living systems with slowing dynamics. This approach has proven useful in framing observations of cellular-scale collective behaviors,[4,11,61] however has not been applied to macroscopic collective systems. The main motivating feature of glass-transition physics is to determine not only the point of collective motion arrest, but the dynamics of the approach to arrest as well.

We observed increasing length and time-scales associated with aggregations during traffic (Fig. 7) and hypothesized that aggregations were the result of repulsive physical interactions due to crowding within the tunnel, and short time delays between interacting ants as they paused to antennate. The probability distribution of spatial aggregations displayed an exponential tail (Fig. 5), which has been previously observed during the formation of heterogeneous immobile regions in glass formation.[53,54]

A primary interest in glassy materials is the dynamics of the approach to the glass transition. The sensitivity of the system's relaxation time (τ^* in this case) with increasing density (or decreasing temperature for molecular and polymeric glasses) distinguishes two extremes of glassy behavior. In a strong glassy system, τ^* increases exponentially (referred to as Arrhenius scaling) with increasing density on approach to the glass transition. In a fragile glassy system, τ^* increases slowly (slower than exponential, *i.e.* non-Arrhenius) over a broad range of densities until a critical density is reached at which point τ^* increases rapidly (super-exponential).[58]

We may thus ask the question what type of glass transition is experienced by trafficking ants? Fragile glass-like behavior of the ants in simulation has the physical interpretation that traffic may flow smoothly as density increases up to a specific density, at which point the traffic comes to an abrupt slow-down or complete halt (Fig. 9a and b). Further increases in density result in a super-exponential slow-down in relaxation dynamics and the system rapidly comes to a halt. Thus, traffic flow that is similar to fragile glassy phenomena will flow smoothly as long as the arrest density is avoided. In the case of strong glassy behavior, increasing density across a wide range of densities results in an exponential increase in traffic flow time-scales (Fig. 9c). In the case of strong-glassy arrest dynamics the ants would be subject to rapid slowing of traffic over a wide range of densities.

We measured system relaxation dynamics as a function of social-interaction time, from no social-interaction time (T_{int} = 0 s) to an extremely large social interaction time (T_{int} = 60 s, well above the observed interaction time of $T_{int} = 0.45 \pm 0.26$ s). We found that by increasing the social-interaction times, from asocial to highly social, the relaxation time-scale *versus* density curves changed from fragile (sharply increasing at a critical density) to strong (varying smoothly with increasing density) relaxation dynamics as shown in Fig. 9c.

By making an analogy with non-living high density systems, we can motivate why ant traffic displays features of a fragile glass-transition. In supercooled liquids which form fragile

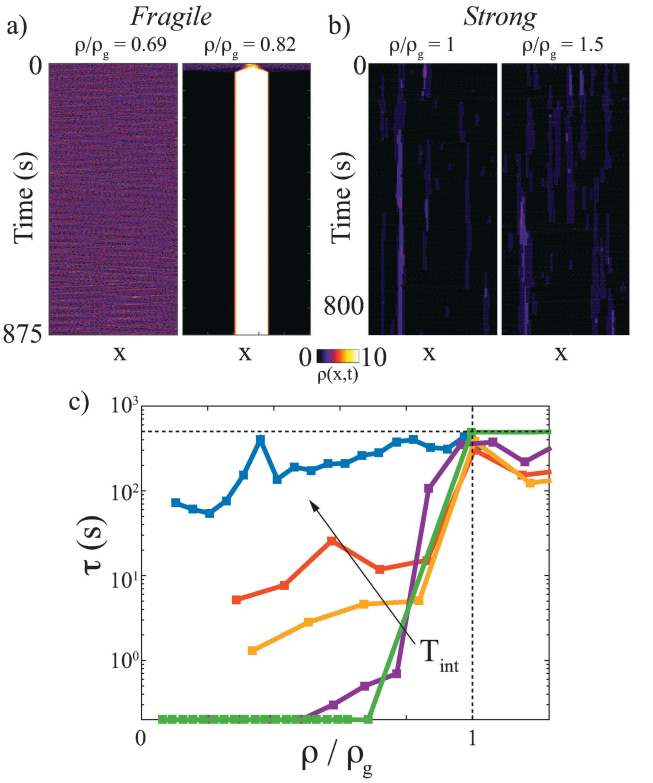

Fig. 9 Strong and fragile behavior of simulated traffic. (a) Space-time traffic flow for T_{int} = 0.1 s simulations at two densities near the arrest transition. Colors in both a and b represent magnitude of $\rho(x,t)$. (b) Space-time traffic flow for T_{int} = 60.7 s simulations at two densities below (left) and above (right) the arrest transition. (c) Relaxation time *versus* density plot illustrating the glass transition dynamics. Note the logarithmic vertical axis. Density has been normalized the glass transition densities. Interactions times from upper to lower are T_{int} = 60.7, 12.2, 6.1 1.2, 0.1 s. The observed biological interaction time in tunnels 3 mm and larger was $T_{int} = 0.45 \pm 0.26$ s (see Fig. 2d).

glasses, molecules interact weakly and non-directionally, while for strong glasses the interactions are the result of large-scale networks of strong covalent bonds.[58] In colloidal and hard-sphere systems a crossover from fragile to strong glass formation is observed as the stiffness of the particles is decreased.[22,62] Hard-sphere systems with short-range interactions like granular materials exhibit fragile behavior,[62] similar to the ants. The fragility of hard-sphere systems is thought to originate from the fact that single-particle rearrangements at high-density require the corresponding motion of large regions surrounding the particles (dynamical heterogeneities), whereas for soft particles, rearrangements can be accommodated through the compression of nearby particles. Thus hard-sphere systems can support minimally obtrusive particle rearrangements until a critical density is reached at which point large volumes of the material must be moved to support rearrangements.

We observed that collective ant traffic is the result of local interactions, which give rise to the fragile nature of collective ant traffic arrest. These observations are consistent with arrest behavior in inert systems that interact through close-range potentials (*i.e.* granular materials and hard colloids). In the

Published on 02 June 2015. Downloaded by Georgia Institute of Technology on 24/08/2015 18:36:11.

case of ant traffic, fragile dynamics may be advantageous for these organisms since smooth traffic flow is assured over a broad range of densities as long as the critical arrest density is avoided. Furthermore, remaining insensitive to traffic fluctuations over a range of densities may allow for behavioral mechanisms to avoid critical tunnel densities. For instance, ants may be able to avoid critical tunnel densities by counting antennation events in a tunnel and basing decisions of motion on the frequency of these events. Similar interaction-counting based behavioral mechanisms have been shown to regulate decisions to forage in seed harvester ants.[49]

The social-nature of the flow dynamics suggests a new mechanism for the transition from strong to fragile glassy behavior in driven systems. The discrete pauses that accompany ant–ant interactions within the tunnel are similar to the finite contact time and loss of energy that occurs in granular inelastic collapse[63,64] which leads to clustering in dissipative granular systems. We may expect to observe similar phenomena in active matter particulate systems with tunable particle–particle correlation times. Thus, through the study of collective motion and collective behavior in complex living systems like social-insects, we may usher in a new form of active matter, the smart-particle or ''smarticle'', which can tunably avoid or seek jamming phenomena based on the scenario.

4 Conclusion

We found that social-interactions and physical obstruction during foraging traffic of fire ant colonies lead to traffic aggregations and jams. Our experiments and model revealed that the social interactions among worker ants in a tunnel lead to traffic-arrest dynamics similar to that of a hard-sphere, fragile glassy system. The fragile nature of ant traffic arrest was due to the short, finite-time delays on motion induced by social-interactions. We found through simulation that if time-delays of social-interaction are increased, traffic flow dynamics changed to that of a strong glassy system over which traffic jam times steadily increased. Having the character of a fragile glassy system may be advantageous for a collective animal group as the agents would be relatively insensitive to jamming over a broad range of traffic densities. Thus, only traffic densities above a threshold would jam, and thus organisms could regulate traffic to stay below this threshold.

The diversity of collective behavior in nature is broad, and thus searching for universal descriptions of collective living systems poses many challenges. However, the language and tools of soft-matter and glass-transition physics have proven useful in providing a framework in which to discuss and understand collective living systems.[4,37,65] While we have described how collective motion of fire ants arrests, there are many open questions as to how other collective living systems with potentially long-range interactions (like bird flocks or fish schools) might arrest. The insight we have gained into collective locomotion in crowded environments may be used for the design of artificial robotics systems to collectively navigate disaster zones, extra-terrestrial environments, or the natural world.

Acknowledgements

We acknowledge Gregg Rodriguez for help with preliminary experiments. Funding for N.G., D.I.G., and M.A.D.G. provided by NSF PoLS #0957659 and #PHY-1205878 and for D. I. G. also by ARO #W911NF-13-1-0347.

References

1 T. Vicsek and A. Zafeiris, *Phys. Rep.*, 2012, **517**, 71–140.
2 L. Conway, D. Wood, E. Tüzel and J. L. Ross, *Proc. Natl. Acad. Sci. U. S. A.*, 2012, **109**, 20814–20819.
3 S. Vedel, S. Tay, D. M. Johnston, H. Bruus and S. R. Quake, *Proc. Natl. Acad. Sci. U. S. A.*, 2013, **110**, 129–134.
4 T. E. Angelini, E. Hannezo, X. Trepat, M. Marquez, J. J. Fredberg and D. A. Weitz, *Proc. Natl. Acad. Sci. U. S. A.*, 2011, **108**, 4714–4719.
5 H. P. Zhang, A. Be'er, E.-L. Florin and H. L. Swinney, *Proc. Natl. Acad. Sci. U. S. A.*, 2010, **107**, 13626–13630.
6 A. Cavagna, A. Cimarelli, I. Giardina, G. Parisi, R. Santagati, F. Stefanini and M. Viale, *Proc. Natl. Acad. Sci. U. S. A.*, 2010, **107**, 11865–11870.
7 M. Ballerini, N. Cabibbo, R. Candelier, A. Cavagna, E. Cisbani, I. Giardina, A. Orlandi, G. Parisi, A. Procaccini, M. Viale and V. Zdravkovic, *Anim. Behav.*, 2008, **76**, 201–215.
8 I. D. Couzin and J. Krause, *Advances in the Study of Behavior*, Academic Press, 2003, vol. 32, pp. 1–75.
9 M. Ballerini, N. Cabibbo, R. Candelier, A. Cavagna, E. Cisbani, I. Giardina, V. Lecomte, A. Orlandi, G. Parisi, A. Procaccini, M. Viale and V. Zdravkovic, *Proc. Natl. Acad. Sci. U. S. A.*, 2008, **105**, 1232–1237.
10 U. Lopez, J. Gautrais, I. D. Couzin and G. Theraulaz, *Interface Focus*, 2012, **2**, 693–707.
11 A. J. Kabla, *J. R. Soc., Interface*, 2012, **9**, 3268–3278.
12 S. P. Hoogendoorn and W. Daamen, *Transport. Sci.*, 2005, **39**, 147–159.
13 D. Helbing, *Rev. Mod. Phys.*, 2001, **73**, 1067–1141.
14 A. Garcimartín, J. M. Pastor, L. M. Ferrer, J. J. Ramos, C. Martín-Gómez and I. Zuriguel, *Phys. Rev. E: Stat., Nonlinear, Soft Matter Phys.*, 2015, **91**, 022808.
15 A. S. de Wijn, D. M. Miedema, B. Nienhuis and P. Schall, *Phys. Rev. Lett.*, 2012, **109**, 228001.
16 A. S. Keys, A. R. Abate, S. C. Glotzer and D. J. Durian, *Nat. Phys.*, 2007, **3**, 260–264.
17 O. Dauchot, G. Marty and G. Biroli, *Phys. Rev. Lett.*, 2005, **95**, 265701.
18 K. N. Pham, A. M. Puertas, J. Bergenholtz, S. U. Egelhaaf, A. Moussaïd, P. N. Pusey, A. B. Schofield, M. E. Cates, M. Fuchs and W. C. K. Poon, *Science*, 2002, **296**, 104–106.
19 Z. Cheng, J. Zhu, P. M. Chaikin, S.-E. Phan and W. B. Russel, *Phys. Rev. E: Stat., Nonlinear, Soft Matter Phys.*, 2002, **65**, 041405.
20 I. Theurkauff, C. Cottin-Bizonne, J. Palacci, C. Ybert and L. Bocquet, *Phys. Rev. Lett.*, 2012, **108**, 268303.
21 E. R. Weeks, J. C. Crocker, A. C. Levitt, A. Schofield and D. A. Weitz, *Science*, 2000, **287**, 627–631.

 This journal is © The Royal Society of Chemistry 2015

Published on 02 June 2015. Downloaded by Georgia Institute of Technology on 24/08/2015 18:36:11.

22 J. Mattsson, H. M. Wyss, A. Fernandez-Nieves, K. Miyazaki, Z. Hu, D. R. Reichman and D. A. Weitz, *Nature*, 2009, **462**, 83–86.
23 P. Chaudhuri, L. Berthier and W. Kob, *Phys. Rev. Lett.*, 2007, **99**, 060604.
24 P. G. Debenedetti and F. H. Stillinger, *Nature*, 2001, **410**, 259–267.
25 A. C. Pan, J. P. Garrahan and D. Chandler, *Phys. Rev. E: Stat., Nonlinear, Soft Matter Phys.*, 2005, **72**, 041106.
26 M. Burd and N. Aranwela, *Insectes Soc.*, 2003, **50**, 3–8.
27 S.-H. Lee, P. Bardunias and N.-Y. Su, *Behav. Processes*, 2008, **77**, 135–138.
28 P. M. Bardunias and N.-Y. Su, *J. Insect Behav.*, 2010, **23**, 189–204.
29 M. Muramatsu, T. Irie and T. Nagatani, *Phys. A*, 1999, **267**, 487–498.
30 W. Daamen, S. Hoogendoorn and P. Bovy, *Transp. Res. Rec.*, 2005, **1934**, 43–52.
31 A. Seyfried, B. Steffen, W. Klingsch and M. Boltes, *J. Stat. Mech.: Theory Exp.*, 2005, **2005**, P10002.
32 W. Daamen and S. Hoogendoorn, *Transp. Res. Rec.*, 2003, **1828**, 20–30.
33 S. Tewari, M. Dichter and B. Chakraborty, *Soft Matter*, 2013, **9**, 5016–5024.
34 B. Hölldobler and E. O. Wilson, *The Ants*, Belknap Press of Harvard University Press, 1990.
35 G. P. Markin, J. O'Neal and J. Dillier, *J. Kans. Entomol. Soc.*, 1975, **48**, 83–89.
36 J. S. Turner, *The extended organism: the physiology of animal-built structures*, Harvard University Press, 2009.
37 M. Sadati, A. Nourhani, J. J. Fredberg and N. Taheri Qazvini, *Wiley Interdiscip. Rev.: Syst. Biol. Med.*, 2014, **6**, 137–149.
38 R. Ni, M. A. Cohen Stuart and M. Dijkstra, *Nat. Commun.*, 2013, **4**, 2704.
39 B. Blonder and A. Dornhaus, *PLoS One*, 2011, **6**, e20298.
40 W. R. Tschinkel, *The fire ants*, Harvard University Press, 2006.
41 D. Monaenkova, N. Gravish, G. Rodriguez, R. Kutner, M. A. D. Goodisman and D. I. Goldman, *J. Exp. Biol.*, 2015, **218**, 1295.
42 V. Fourcassié, A. Dussutour and J.-L. Deneubourg, *J. Exp. Biol.*, 2010, **213**, 2357–2363.
43 A. John, A. Schadschneider, D. Chowdhury and K. Nishinari, *Phys. Rev. Lett.*, 2009, **102**, 108001.
44 M. Burd, D. Archer, N. Aranwela and D. J. Stradling, *Am. Nat.*, 2002, 283–293.
45 I. D. Couzin and N. R. Franks, *Proc. Biol. Sci.*, 2003, **270**, 139–146.
46 A. Dussutour, S. C. Nicolis, J.-L. Deneubourg and V. Fourcassié, *Behav. Ecol. Sociobiol.*, 2006, **61**, 17–30.
47 A. Dussutour, J.-L. Deneubourg and V. Fourcassié, *J. Exp. Biol.*, 2005, **208**, 2903–2912.
48 M. Burd, *Phys. A*, 2006, **372**, 124–131.
49 F. R. Adler and D. M. Gordon, *Am. Nat.*, 1992, **140**, 373–400.
50 D. Cassill, *Behav. Ecol. Sociobiol.*, 2003, **54**, 441–450.
51 J. L. Breton and V. Fourcassié, *Behav. Ecol. Sociobiol.*, 2004, **55**, 242–250.
52 J. Zhang and A. Seyfried, *Procedia Eng.*, 2013, **62**, 655–662.
53 A. Patti, D. El Masri, R. van Roij and M. Dijkstra, *Phys. Rev. Lett.*, 2009, **103**, 248304.
54 C. Donati, J. F. Douglas, W. Kob, S. J. Plimpton, P. H. Poole and S. C. Glotzer, *Phys. Rev. Lett.*, 1998, **80**, 2338–2341.
55 K. N. Nordstrom, J. P. Gollub and D. J. Durian, *Phys. Rev. E: Stat., Nonlinear, Soft Matter Phys.*, 2011, **84**, 021403.
56 N. Lačević, F. W. Starr, T. B. Schrder and S. C. Glotzer, *J. Chem. Phys.*, 2003, **119**, 7372–7387.
57 H. Katsuragi, A. R. Abate and D. J. Durian, *Soft Matter*, 2010, **6**, 3023–3029.
58 M. D. Ediger, C. A. Angell and S. R. Nagel, *J. Phys. Chem.*, 1996, **100**, 13200–13212.
59 W. R. Tschinkel, *J. Insect Sci.*, 2011, **11**, 26.
60 N. Gravish, D. Monaenkova, M. A. D. Goodisman and D. I. Goldman, *Proc. Natl. Acad. Sci. U. S. A.*, 2013, **110**, 9746–9751.
61 S. R. K. Vedula, M. C. Leong, T. L. Lai, P. Hersen, A. J. Kabla, C. T. Lim and B. Ladoux, *Proc. Natl. Acad. Sci. U. S. A.*, 2012, **109**, 12974–12979.
62 P. M. Reis, R. A. Ingale and M. D. Shattuck, *Phys. Rev. Lett.*, 2007, **98**, 188301.
63 S. McNamara and W. R. Young, *Phys. Rev. E: Stat. Phys., Plasmas, Fluids, Relat. Interdiscip. Top.*, 1994, **50**, R28–R31.
64 S. McNamara and W. R. Young, *Phys. Rev. E: Stat. Phys., Plasmas, Fluids, Relat. Interdiscip. Top.*, 1994, **50.1**, R28.
65 L. Berthier, *Phys. Rev. Lett.*, 2014, **112**, 220602.